An experimental study of vertical greenery systems for window shading for energy saving in summer

Zheng, Xing; Dai, Tianchen; Tang, Mingfang

Important note
To cite this publication, please use the final published version (if applicable).
Please check the document version above.

An experimental study of vertical greenery systems for window shading for energy saving in summer

Xing Zheng [1], Tianchen Dai [2], Mingfang Tang [1]

[1] Faculty of Architecture and Urban Planning, Chongqing University, Chong Qing City, 400045, PR China
[2] Faculty of Architecture and the Built Environment, Delft University of Technology, 2600AA Delft, The Netherlands

Abstract:

Past studies have demonstrated the remarkable energy-saving effect of vertical greenery systems. The vast majority of these works focus on opaque building walls. While external shadings on windows are more effective than these on walls. Inspired by the climbing plants (vines) raised outside windows by residents, the present study proposed the design of movable green window shading systems (MGWSS) that can shade beam solar radiation but allows soft daylighting. On the basis of simplified MGWSS models, experiments were conducted in summer to evaluate the shading performance with three plant species. First, the energy-saving effect and climatic data were measured for test rooms with west-facing windows. The results indicated that the presence of green shading reduced the impact of solar radiation on the cooling energy consumption with the correlation coefficients from 0.94 to 0.61. Then, the shading coefficient, which is a key parameter for energy saving, was measured by a new technique using photovoltaic panels. The correlation between the coverage rate and the surface-averaged shading coefficient was established. The results showed that when the coverage rate of the MGWSS with Dishcloth gourd was 80%, the shading coefficient was 0.28, and the cooling energy consumption and heat flux transferred through the window glass were reduced by 11.5% and 64.8%, respectively. The shading characteristic was investigated using the instantaneous data. It found that stronger ambient solar radiation resulted in better shading performance (lower shading coefficient). For a west-facing window, the best shading performance was found at oblique solar incidence angles.

Keywords: Shading coefficient; Vegetative; Vertical greening; Green façade; Energy saving; Solar shading system

Nomenclature:

C_c	Correlation coefficients
C_s	Shading coefficients
$C_{s.loc}$	Local shading coefficients
$C_{s.s.avg}$	Surface-averaged shading coefficients
C_r (%)	Coverage rate (by percentage)

Q	Heat transfer through building envelops
F (m²)	Heat transfer surface area
SHGC	Solar heat gain coefficients
U (W/(m²K))	Heat transfer coefficients
T_e (°C)	Ambient air temperature
T_i (°C)	Indoor air temperature
h_e (W/(m²K))	External surface heat transfer coefficient
ρ	Solar radiation absorptivity
E (W/m²)	Solar radiation
E_i (W/m²)	Solar radiation behind the green shading
E_a (W/m²)	Ambient solar radiation on a vertical surface
E_r	Total solar radiation on the roof surface
V (V)	Voltage
α (°)	Solar altitude angle
β (°)	The angle between the west and the solar azimuth angle
SD	Standard deviation

1. Introduction

Building greenery systems provide many environmental benefits to cities, such as improvement in thermal comfort (Imran et al., 2018; Susorova et al., 2014) and air quality (Abhijith et al., 2017), reduction of building overheating and energy usage (Alexandri and Jones, 2008; Huang et al., 2019) (Tang and Zheng, 2019), and enhancement of urban landscape aesthetic. In particular, past studies demonstrated that vertical greenery systems can considerably cool the surface of the building envelope and reduce building cooling load in summer.

In recent overviews on developments of vertical greenery systems (Bustami et al., 2018; Pérez et al., 2014a; Safikhani et al., 2014; Zaid et al., 2018), vertical greenery systems are divided into two main categories: living walls and green facades. Living walls are constructed from modular panels that contain soil or other artificial growing mediums (De Masi et al., 2019; Feng and Hewage, 2014; Perini et al., 2013), while green facades are based on climbing plants that rooted in the ground (Perini and Rosasco, 2013). Compared to living walls, green façades have the advantage that they could cover not only the façade opaque area but also the windows (Pérez et al., 2014a). External shading on windows is a key design feature for energy saving (Ebrahimpour and Maerefat, 2011; Haldi and Robinson, 2010; Hamdan, 1994; Kirimtat et al., 2016), which is more effective than shading on walls. However, the vast majority of the experimental studies have focused on vertical green systems for opaque building walls without openings. Only a few studies explored its application for windows (Ip et al., 2004; Sunakorn and

Yimprayoon, 2011). In addition, these greenery shading devices for windows were heavy and not movable, which limit their application. Thus, there is a great need for more research into the potential for using vegetation for window shading.

The present study proposes a design of movable green window shading systems (MGWSS). Simplified models of MGWSS were built for experimental use. Three plant species were evaluated. A new technology using PV panels was developed to measure the shading performance. The reduction of cooling energy consumption by MGWSS was studied, and the correlation between the shading coefficient and coverage ratio was established. The rest of the paper is organized as follows. Section 2 starts from the literature on the thermal performance of green facades, then an overview of green shading for windows is presented. Section 3 introduces the design of MGWSS, measurement technique and the experimental steps. Section 4 analyzes the measured results. Discussion and limitations are presented in Section 5 and finally, Section 6 provides conclusions.

2. Literature review

More papers on general green facades have been found than specific on windows. Since they do share some similar features in perspectives of mechanism, research on green facades is also useful for investigation on windows. Thus a review starts from the thermal performance of green façades.

2.1 Thermal performance of green facades

Many studies reported that green facades could reduce the surface temperature behind (Cuce, 2017; G. Pérez et al., 2011; Stec et al., 2005; Wong et al., 2010) and heat flux (Sudimac et al., 2019; Susorova et al., 2014) that transferred through the building envelope. Past studies showed the main cooling mechanism is the interception of solar radiation produced by the plant canopy (Hoelscher et al., 2016; Koyama et al., 2015; Papadakis et al., 2001; Gabriel Pérez et al., 2011; Yang et al., 2017). Compared with conventional shading material such as metal or plastic, plants have an extra function of transpiration and could maintain a low surface temperature under the sun. While conventional material can have high surface temperature and impose strong heat radiation into the interior space. For example, Stec et al. (Stec et al., 2005) examined the thermal performance of a double-glazed façade with live plants and shading blinds in the cavity, the increase of the back wall surface temperature with plants was found to be 20% lower than that with shading blinds.

The thermal performance of green façades depends on many factors such as the orientation (Jim, 2015; Pan et al., 2018), the plant characteristic, and the construction of green façades. An experimental study conducted in Hong Kong indicated a west-facing green facade had the highest capacity in the surface temperature reduction (Pan et al., 2018). Experimental studies performed in Greece (Eumorfopoulou and Kontoleon, 2009; Kontoleon and Eumorfopoulou, 2010) proved that the influence

of a green cover on the wall surface was pronounced for east-oriented and west-oriented surfaces. Similar results were found in Chicago, USA (Susorova et al., 2014).

Another important factor that affects the thermal performance of green facades is the plant characteristic, which is mainly the density of the foliage. One of the indexes to characterize the density of the foliage is the Leaf area index (LAI). Traditionally, the concept of LAI has been used in agriculture and its calculation was done in horizontal (Pérez et al., 2014a). For a vertical green facade, the LAI was widely estimated as the projected area of leaves per unit area of the vertical wall surface. Another index broadly applied to characterize the canopy foliage density was coverage rate (C_r), which was the percentage of the area covered by plants to the total area (Koyama et al., 2013). Compared with LAI, C_r is easier to be measured. Kontoleon and Eumorfopoulou (Kontoleon and Eumorfopoulou, 2010) found that the indoor air temperature decreased with the increase of C_r for a building with a green facade. Koyama et al. (Koyama et al., 2013) investigated five vine plant species located on freestanding walls and found that the C_r was the key trait reducing the wall surface temperature. Significant positive relationships between the C_r and the temperature reduction by the green screens were found, ranging from 3.7 °C to 11.3 °C, with the C_r from 15% to 54%. These studies demonstrated that the thermal performance of the green facade is highly depended on C_r.

The thermal performance of green façades also depends on its construction, which can be categorized into two types: traditional green façades and double-skin green façades (Pérez et al., 2014a). Traditional green façades are the ones in which plants are attached to the walls directly. While double-skin green façades, namely indirect green façades in a few literature (Bustami et al., 2018; Perini et al., 2011), have an extra vertical support structure for climbing plants, therefore, cover the façades but separated from building walls (Ling and Chiang, 2018; Pérez et al., 2014a). Perini et al. (Perini et al., 2011) found that a double-skin green façade reduced the building's exterior surface temperature by 2.7 °C, which was 1.5 °C more than a traditional green facade. Moreover, the double-skin green façades have the advantage that they could also cover windows (Pérez et al., 2014a).

2.2 Greenery shading for windows

An experimental study (Sunakorn and Yimprayoon, 2011) using climbing plants as a vertical window shading for a natural ventilated building showed that the difference of indoor air temperature between the test room with green shading and the reference room without shading was 4.71 °C at maximum, and 0.89 °C on average in a daytime. Another experiment on green shading for windows demonstrated a reduction of peak summer temperature by 4–6 °C (Ip et al., 2004). These studies evaluated the passive cooling effect by green shading on windows; however, the energy-saving effect has not yet been measured.

Shading coefficient (C_s) is an index that represents the proportion of the solar radiation received in front of the shading to the solar radiation received behind (Chartered Institution of Building Services Engineers., 2006). It has been widely used to evaluate the window shading devices for building thermal design. For common shading devices made of metal or wood with fixed geometry, the solar gain behind the shading devices can be calculated (Palmero-Marrero and Oliveira, 2010; Singh et al., 2016) and the corresponding C_s can be obtained (David et al., 2011). However, this is not the case for vertical green systems because of the free grown shape of the canopy. Existing numerical studies have made assumptions on the value of the shading coefficient for vertical green systems (Pérez et al., 2014b; Susorova et al., 2013). For example, a numerical study (Wong et al., 2009) assumed the shading coefficient of the green coverage of 0.041, and it found that the greenery coverage reduced the envelope thermal transfer value of a glazed building by 40.68%. A direct way to evaluate the shading performance of plants is on-site measurement (G. Pérez et al., 2011; Gabriel Pérez et al., 2011; Pérez et al., 2014a). Lp et al. (Ip et al., 2010) performed a pioneer experimental study on C_s for windows shading by climbing plants. The solar radiation in front and behind the green shading was measured by pyranometer (solar flux sensors) for one year. The measured data were applied to establish the shading coefficient function, which represented the seasonal variation of shading performance during the biological cycle of an entire year.

The extant literature above indicates research gaps related to green shading for windows mainly in three aspects: (1) The shading effect from the green canopy can vary locally and be inhomogeneous because of foliage characteristics. In the past, solar radiation behind window green shading has been measured by points with pyranometers or radiometers (Ip et al., 2010), which could not capture either the surface-averaged or the distribution of solar radiation behind the green shading. Developments of new measurement techniques are needed. (2) Past studies on green facades have shown the relationship between C_r and surface cooling effect for oblique walls, while C_s is a fundamental index for window shading performance. Correlation between C_r and C_s has not yet been investigated. (3) Past study on the cooling energy-saving effect by window green shading was based on numerical simulations with assumed values of C_s (Wong et al., 2009). Experimental evaluation of the cooling energy-saving effect has not yet been conducted.

3. Material and method

3.1 Plant species

Suitable plant species are important in enhancing the energy benefits of vertical greeny systems (Dahanayake et al., 2017). In the present study, the species were selected based on the literature and also our local observation. Fig. 1 shows the climbing plants raised outside windows by local residents in Chongqing. Chongqing is located in the hot-summer-cold-winter region in southwest China (29.6N,

106.5E). As the extreme air temperature in summer could reach 43 °C, the solar shading effect of these "self-built green shading" is considerable during sunny summer days. Dishcloth gourd (Figs. 1a and b) and Morning glory (Fig. 1c) are the main species raised by local residents that observed in Chongqing city. They can shade the beam solar radiation and dazzle but allow soft day lighting. Moreover, Dishcloth gourd was examined as a shading material for vine sunscreen in an experimental study (Hoyano, 1988). Morning glory has been widely used for green façades in Asia (Koyama et al., 2013). Another species commonly found in southwest China is Malabar spinach, which can be used as vegetables and traditional Chinese medicine. In the present study, the three species: Morning glory, Malabar spinach, and Dishcloth gourd were selected as shading plants.

Fig. 1. Climbing plants raised outside windows by residents: (a–b) Morning glory and (c) Dishcloth gourd.

3.2 Design of MGWSS and simplified models

As stated before, most of the existing green shading devices were fixed and not movable, which limits their application. To improve the adjustability and movability, we designed movable green window shading systems (MGWSS). Two types of MGWSS are shown in Figs. 2a and b, respectively. Both systems are fixed to building walls with supporting frameworks made of aluminum alloy. Lightweight planting technology provides the possibility of a constructive solution for window shading using vegetation. Type A slides horizontally, whereas type B slides vertically. The detailed construction of type A is illustrated in Figs. 2c and d. The main component of MGWSS (type A) is a sliding planting module, which can slip on a track to switch from shading to un-shading. The sliding planting module includes a lightweight planter box and a single-layer wire net. The lightweight planter has substrates inside, and the plant is supported by the wire net. An irrigation system is connected to the planter box.
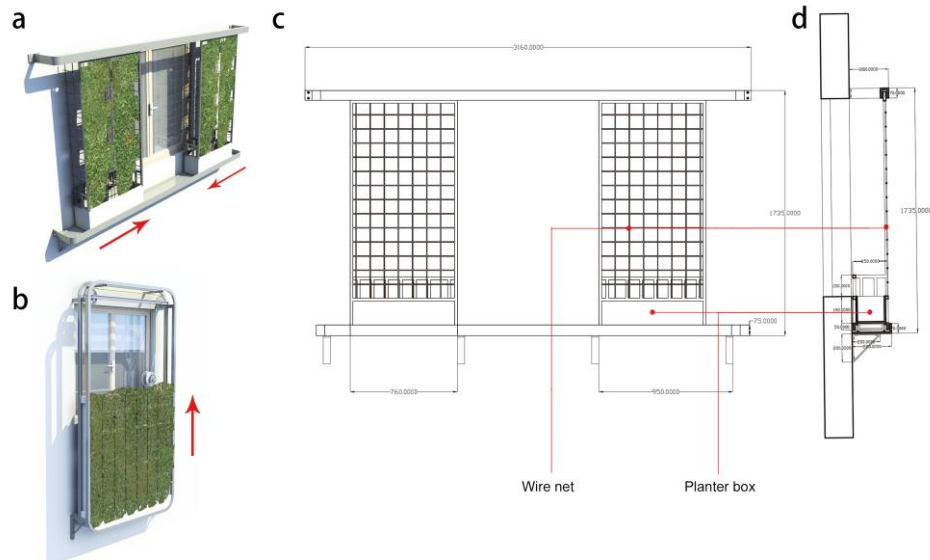
Fig. 2. Movable green window shading systems: (a) type A, (b) type B, (c) detailed drawing of type A, and (d) section drawing of type A.

We built simplified models of MGWSS for experimental use. These models of MGWSS were composed of planter boxes and a stainless steel framework with the single-layer supporting net. The simplified models represented the MGWSS at the shading status. The size of the plant supporting net was 1.3 m×1.4 m, which was sufficient to cover a normal window.

In the present experiment, these plants were transplanted into the planter boxes in early July (Figs. 3a-c). Then, they climbed on the net and became green shading materials (Figs. 3d-f).
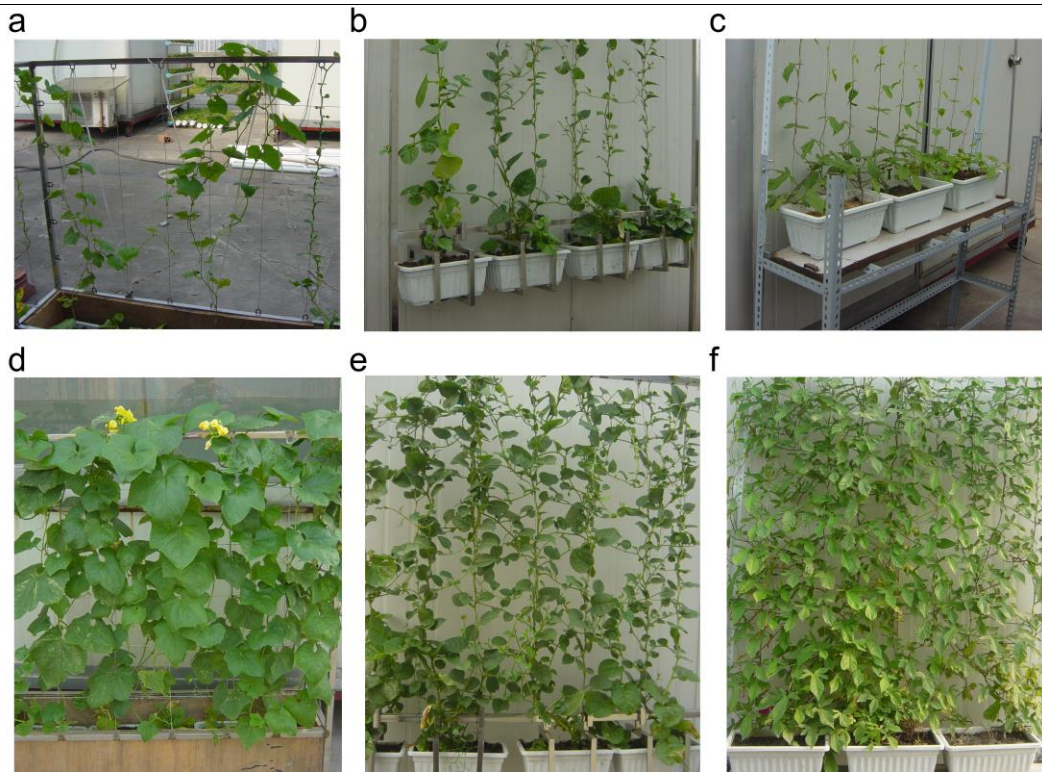
Fig. 3. Plants in the simplified models of MGWSS in early July: (a) Dishcloth gourd (b) Malabar spinach, (c) Morning glory, and (d)–(f) same in August.

3.3 Experimental site

The experiment was conducted on the building roof of the Faculty of Architecture and Urban Planning in Chongqing University campus (29.6°N, 106.5°E), Chongqing, China. Two identical lightweight rooms on the roof of the faculty building (Fig. 4a) were used. The windows facing the west and there was no building or object in front. The distance between the two rooms ensured that they would not shade each other in summer days. Each room had a dimension of D × W × H = 2.4 m × 2.4 m× 2.5 m, installed with the same wall-mounted air conditioners. The input power of the air conditioners was 1,080 W, with a cooling capacity of 3,250W. The opaque envelopes of the rooms were constructed by thermal insulation sandwich boards, made of polyethylene foam (conductivity 0.042 $W^.m^{-1.}K^{-1}$). The total thickness of the wall and roof were 50 mm and 100 mm, respectively. The heat transfer coefficients of the wall and the roof were 0.75 $W^.m^{-2.}K^{-1}$ and 0.40 $W^.m^{-2.}K^{-1}$ respectively. The windows of both rooms had a size of 1.2 m × 1.2 m, composed of 6 mm single pane clear glass (SHGC (Solar heat gain coefficient) = 0.82, Solar transmittance = 0.93, thermal transmittance 5.7 = $W^.m^{-2.}K^{-1}$).

Note that the model was not fixed on the window. When the MGWSS models were placed in front of the window, soft daylight and preferable interior visual views were achieved (Fig. 4b).
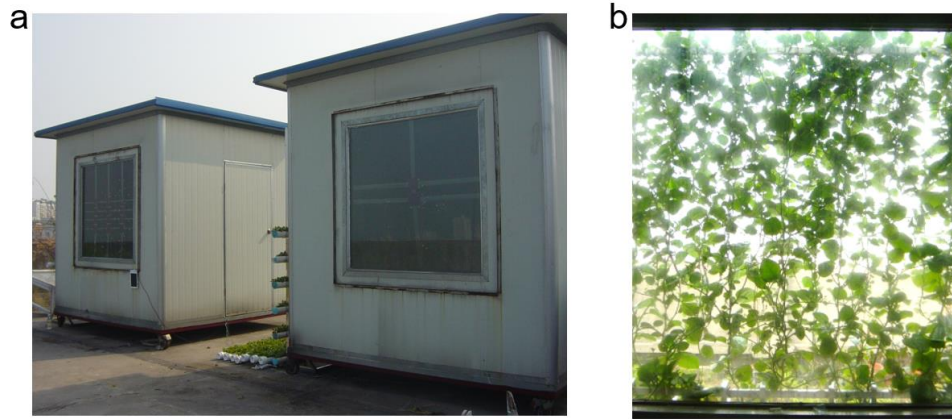
Fig. 4. (a) Lightweight rooms and (b) interior view of Malabar spinach shading.

3.4 Measurement step

Three main experiments were planned: (1) Experiment of cooling energy consumption and heat flux for the west-facing windows (detailed in 3.4.1), in which the cooling energy consumption and heat flux transferred through the window glass were measured simultaneously. (2) The experiment of shading coefficient for the west-facing windows (detailed in 3.4.2), in which the ambient solar radiation and the local solar radiation behind the green shading were measured to quantify the shading coefficient. (3) Solar tracking experiment of shading coefficient (detailed in 3.4.3). Experiments (1) and (2) were for the west-facing windows since the west is a critical orientation for building glaze. Table 1 lists the details of the equipment used in the three experiments.

Table 1. Instrumental specifications

Equipment	Type	Variable	Accuracy
PV panel	6V80MA	Voltage (V)	-
Pyranometer	S-LIB-M003	Solar radiation (W/m^2)	± 10 W/m^2 or $\pm 5\%$
Data acquisition meter	Agilent 34970A	-	-
Heat flux sensor	WYP	Heat flux (W/m^2))	$\pm 3\%$
Thermocouple	T	Temperatures (°C)	$\pm 0.3°C$

3.4.1 Experiment of cooling energy consumption and heat flux for the west-facing windows

This experiment aims at measuring the cooling energy consumption and heat flux transferred through the window glass. Cooling energy consumption and heat flux were measured by placing the model of MGWSS in front of the test room (Fig. 5a), two species were considered: (1) Dishcloth gourd and (2) Malabar spinach. Two reference conditions were considered: (1) window without shading and (2) window fully covered with a louver shading (Fig. 5c). For the window without shading, the C_s can

9

be considered as 1. The window fully covered with louver shading represents the maximum shading effect with C_s of 0.

Due to the presence of green canopy, some parts of the glass surface may receive more heat flux and some parts may receive less. One heat flux sensor can only measure the heat flux transferred through a small area. To eliminate the potential inhomogeneity, 12 heat flux sensors were pasted in 4 rows and 3 columns on the inner window glass surface (Figs. 5a and b). The size of each sensor was 100 mm×100 mm. The horizontal and vertical distances between the two sensors were 120 mm and 40 mm. The results were averaged from the 12 sensors and reported in reminders of this paper.

To monitor the indoor air temperature, thermocouples were situated at the center of the rooms. All the heat flux sensors and thermocouples were connected with a 34970A data acquisition system, and the data were collected every 1 min. A weather station was placed on the open area to monitor the outdoor meteorological data.

This experiment was performing in August. During the experiment, the air conditioners were switched on with the set temperature of 22 °C. The cooling energy consumption was recorded during the experiment.
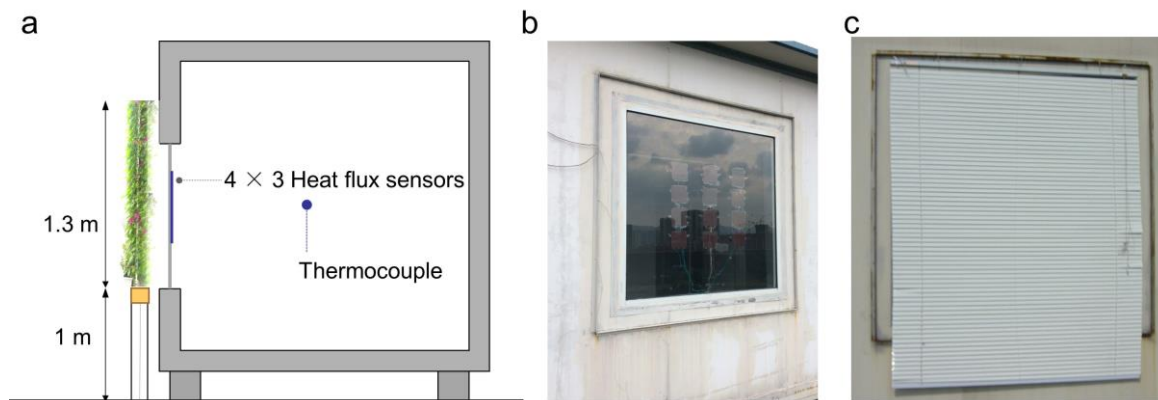

Fig. 5. (a) Construction of the test room, (b) heat flux sensors, and (c) window fully covered with louver shading

Past studies demonstrated that the shading performance was highly correlated with solar radiation. For example, the cooling effect was observed when the solar radiation excessed 100 W/m² (Koyama et al., 2013), and a threshold solar intensity of about 300 W/m² was found to be necessary to impart a notable cooling-effect (Jim, 2015). In summer sunny days, beam solar radiation on the west vertical plane (surface of the west-facing window) starts from around 12:00 PM with the radiation larger than 100 W/m². As the two rooms were constructed of lightweight insulation material with small thermal inertia, the heat flux transferred into the room was generally simultaneous with the cooling energy consumption. Moreover, our test on the reference room showed that 80% of the daily heat flux that

transferred through the window happened during 12:00-18:00 PM. Therefore, the results obtained from 12:00 to 18:00 PM were used for analysis.

3.4.2 Experiment of shading coefficients for the west-facing windows

A new measuring technique was developed using photovoltaic (PV) panels to obtain the local shading coefficient. Given that photovoltaic (PV) panels convert solar energy into electrical energy, solar radiation could be measured by PV panels indirectly. The detail of this technique and a calibration experiment will be presented in section 3.4.4.

A measuring board was made of a PV panel array and a supporting frame. We divided the central area within the frame into 7×5 parts. Then, 35 PV panels were fixed on the frame with taps correspondingly (Figs. 6a and b). The size of each PV panel was 100 mm×60 mm. The horizontal and vertical distances between two PV panels were 20 mm. The PV array on the measuring board could measure the solar radiation in an area of 540 mm×580 mm. Three additional PV panels were installed on the top of the measuring board to measure the ambient solar radiation on the vertical plane (Fig. 7a).
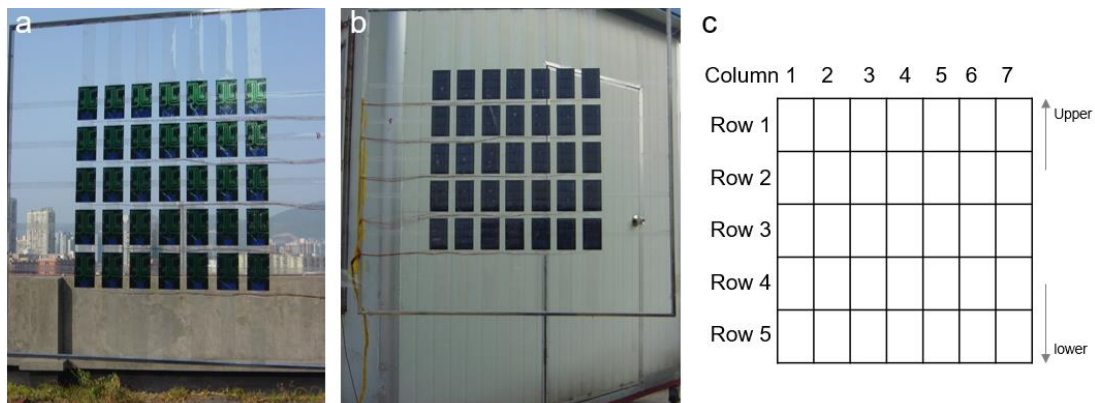

Fig. 6. Measuring board: (a) back, (b) front, and (c) division of the measuring area.

The measuring board was positioned close to the window, ensuring that the PV array would be located near the central area of the window. Then, the model of MGWSS was placed 200 mm in front of the measuring board to guarantee that direct sunlights could not reach the PV array through the lateral gaps (Fig. 7). All the PV panels were connected with the data acquisition system, and the data were collected every 1 min. The experiment was conducted in the afternoon, the data recording started from 13:00 PM and ended after the sunset. The three species were measured alternately in daily rounds from August to October. During the experimental period, the substrate was watered once a day.
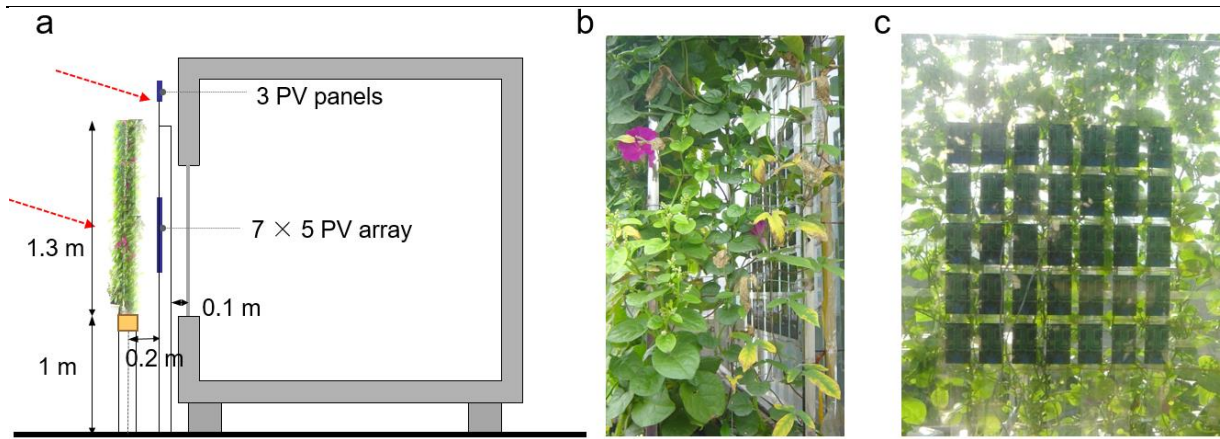
Fig. 7 (a) Construction of the test room and location of PV panels in the experiment for west-facing windows. (b) Side view of the measuring board and the model of MGWSS. (c) Interior view of the measuring board and the model of MGWSS.

3.4.3 Solar tracking experiment of shading coefficient

The solar tracking experiment of the shading coefficient was conducted without fixing the orientation. The goal was to explorer the shading coefficient when the solar azimuth angle is perpendicular to the window. The model of MGWSS was placed in front of the measuring board that mentioned in 3.4.2. We kept the model of MGWSS and the measuring board facing the sun by turning their orientation together by hands every half hour, to keep the board nearly perpendicular to the solar azimuth angle during the measurement. This solar tracking experiment was only performed for Dishcloth gourd from 10:00 AM to 16:00 PM on a sunny day (August 14).

3.4.4 Calibration experiment and conversion of shading coefficients

Photovoltaic (PV) panels convert solar energy into electrical energy. On the basis of the photoelectric effect, the relationship between the solar radiation and the output power of PV cells is expressed in Eq. (1) (Skoplaki and Palyvos, 2009):

$$P = A\eta_c E, \tag{1}$$

where P is the output power, A is the aperture area of PV panel (m^2), and E is the solar radiation. The electrical efficiency η_c is a constant, following the previous study that assumed the familiar linear form (Skoplaki and Palyvos, 2009). Given that the output power of a PV panel can be monitored by the voltmeter, a calibration experiment was conducted to obtain the correlation between the output voltage and the solar radiation. First, we placed a PV panel and a pyranometer at the same height facing the west, therefore, the PV panel and the pyranometer could receive the same solar radiation. Then, we measured the output voltage of each PV panel with a data acquisition instrument on a sunny afternoon.

Synchronously, the solar radiation was recorded by the pyranometer. Then, calibrations were made for each panel at the same time. Fig. 8a shows the linear correlation between solar radiation and the voltage (V) from one of the PV panels. It observed that the solar radiation ranged from 150 W/m^2 to 600 W/m^2 during that afternoon. The voltage (V) from that PV panel and solar radiation from the pyranometer showed a strong positive linear correlation (by the orange dashed line) with R^2 of 0.992. Then, the voltage was converted into solar radiation and compared with the solar radiation from pyranometer in Fig. 8b. For all these panels, the average relative deviation between the solar radiations obtained from PV panels and measured by pyranometer ranged from 1.1% to 5.3%. This calibration experiment proved that PV panels could be used to measure the solar radiation on a surface with acceptable accuracy.
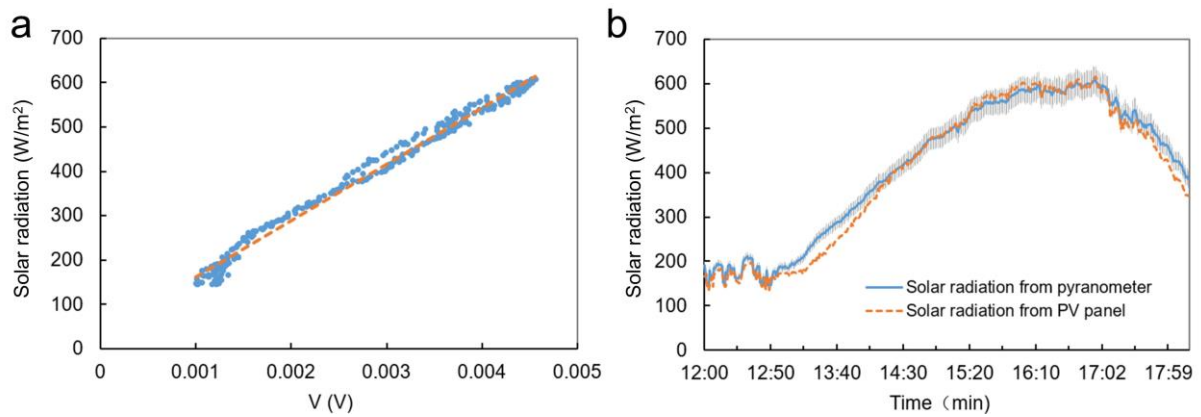

Fig. 8 (a) Linear correlation between voltage (V) from a PV panel and solar radiation from pyranometer and (b) Solar radiation measured by pyranometer and solar radiation calculated from the PV output during the calibration experiment.

On the basis of the linear correlation from the calibration experiment, ambient solar radiation on the vertical plane was converted from the measured voltage (V) from the three additional PV panels installed on the top. The local solar radiation behind the green shading was converted from the PV array. Following the generally accepted definition (David et al., 2011; Ip et al., 2010), local shading coefficient ($C_{s.loc}$) was defined as:

$$C_{s.loc} = \frac{E_i}{E_a}, \tag{2}$$

Where E_a was ambient solar radiation on the surface and E_i was the solar radiation behind the green shading. The surface-averaged shading coefficient ($C_{s.s.avg}$) was calculated by averaging $C_{s.loc}$ from the 35 panels, as defined in Eq. (3)

$$C_{s.s.avg} = \frac{(\sum_{i=1}^{35} E_i)/35}{E_a}, \tag{3}$$

3.4.5 Conversion of coverage rate

A whiteboard was cropped depending on the opening size of the window. We placed the simplified models with plants in front of the whiteboard and took a picture from a far distance. Then, the photos were converted into binary images to identify the coverage rate by percentage (C_r) (Ip et al., 2010; Koyama et al., 2015, 2013). Fig. 9 presents an example. In this way, C_r was measured during the growth of plants.
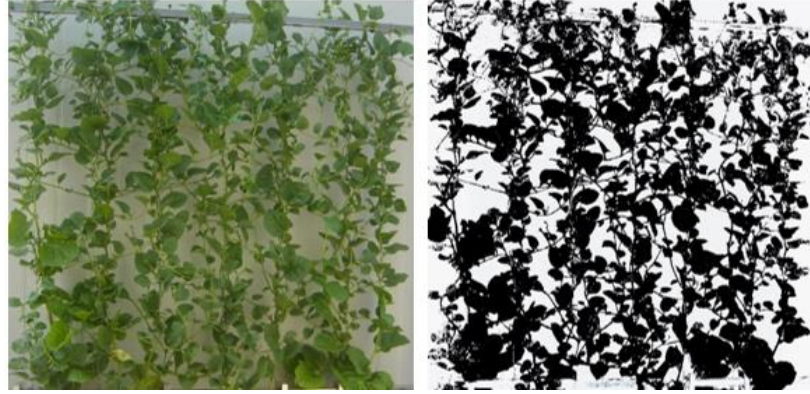

Fig. 9 Conversion of the coverage rate.

4. Results

4.1 Cooling energy saving and reduction of heat flux

In the present experiment, the cooling energy consumption comes from the heat transfer through building envelops (Q), which includes three parts: (1) heat transfer through the roof (Q_{roof}), (2) heat transfer through walls (Q_{wall}), and (3) heat transfer through the window ($Q_{windows}$)：

$$Q = Q_{roof} + Q_{wall} + Q_{window} \tag{4}$$

The heat transfer through the roof (Q_{roof}) can be represented as：

$$Q_{roof} = F_{roof} U_{roof}(\rho E_r/h_e + T_e - T_i) = F_{roof} U_{roof} \rho E_r/h_e + F_{roof} U_{roof}(T_e - T_i) \tag{5}$$

Where, F_{roof} is the heat transfer surface area of the roof; U_{roof} is the heat transfer coefficients of the roof; T_e and T_i is the ambient and indoor air temperature, respectively; E_r is the total solar radiation on the roof surface; ρ is the solar radiation absorptivity, h_e is external surface heat transfer coefficient (W/m²K). Similar, the heat transfer through the walls can be represented as follows:

$$Q_{wall} = U_{wall} \sum_k F_{wall.k} \rho E_{a.k}/h_e + U_{wall}(T_e - T_i) \sum_k F_{wall.k} \tag{6}$$

Where U_{wall} is the heat transfer coefficients of walls; $F_{wall.k}$ is the heat transfer surface area of each wall; $E_{a.k}$ is the total solar radiation incident on the surface of each wall. Heat transfer through the windows can be represented as follows:

$$Q_{window} = F_{window}C_sE_aSHGC + F_{window}U_{window}(T_e - T_i) \qquad (7)$$

Where F_{window} is the heat transfer surface area of the window; SHGC is the solar heat gain coefficient; U_{window} is the heat transfer coefficients of the window; C_s is the window shading coefficients (C_s=1 means window without any shading). Eqs. 5, 6 and 7 indicate that the cooling energy consumption and heat flux not only relate to the two climatic factors (i) indoor-outdoor air temperature difference and (ii) ambient solar radiation, but also the window shading coefficients.

4.1.1 Correlation analyses with climatic factors

The experiment of cooling energy consumption and heat flux for the west windows was conducted in August. As mentioned in 3.4.1, four window conditions are considered: (1) green shading with Dishcloth gourd, (2) green shading with Malabar spinach, (3) fully shading with louver and (4) without shading. Data from 12 discontinuous sunny days are picked out and subsequently averaged on a daily basis between 12:00-18:00 PM. As the cooling energy consumption and heat flux transferred through envelops are related to two climatic factors, correlation analyses with the climatic factors were performed. Figs. 10a b c and d scatter the solar radiation and cooling energy consumption, indoor-outdoor air temperature difference and cooling energy consumption, solar radiation and heat flux, and indoor-outdoor air temperature difference and heat flux, respectively. Tables 2 and 3 summarized the correlation coefficients (C_c) between the cooling energy consumption and climatic factors, and heat flux and climatic factors, respectively. Three scenarios are taken into account: (1) without shading, (2) fully shading with louver and (3) green shading with Malabar spinach. Note that there are only 3 days' data from Dishcloth gourd, therefore, the correlation coefficients are not calculated for green shading with Dishcloth gourd.

For the scenario without shading, the cooling energy consumption was highly correlated with the indoor-outdoor air temperature difference and the ambient solar radiation (Blue points in Figs. 10a and b), with the C_c of 0.92 and 0.94 (Table. 2), respectively. Figs. 10a and c show that cooling energy consumption and heat flux increased dramatically with solar radiation.

The presence of green shading (Malabar spinach and dishcloth gourd) reduced heat flux transferred through the window (Figs. 10c and d). Moreover, it decreased the impact of solar radiation and indoor-outdoor air temperature difference on the cooling energy consumption (Figs. 10a and b). Table 2 shows

that for the room with Malabar spinach shading, the correlation of cooling energy consumption with solar radiation ($C_c = 0.61$) was weaker than with indoor-outdoor air temperature difference ($C_c = 0.79$). Table 3 shows the green shading reduced the impacts of ambient solar radiation and indoor-outdoor air temperature difference on the heat flux. This is not only because it shaded the solar radiation, but also because the temperature of the green canopy was low. Fig. 10a indicates that when the solar radiation was higher than 300 W/m^2, the cooling energy consumption of the room with green shading was always lower than the room without shading, which is in line with a past study (Jim, 2015).

When the window was fully covered by shading louver, the heat flux transferred through the window is significantly reduced (Figs. 10c and d). Table 2 shows that cooling energy consumption was weakly correlated with solar radiation ($C_c = 0.24$), while it was strongly correlated with the indoor-outdoor air temperature difference ($C_c = 0.96$). This is because the C_s of the fully shading equal to 0, therefore, dramatically reduced the impact of solar radiation on cooling energy consumption, and the indoor-outdoor air temperature difference becomes the dominating factor. A bit stronger correlation of heat flux with solar radiation ($C_c = 0.36$) was observed in Table 3. This is because the solar radiation raises the louver surface temperature, therefore, imposes thermal radiation and increases the transmitted heat flux.
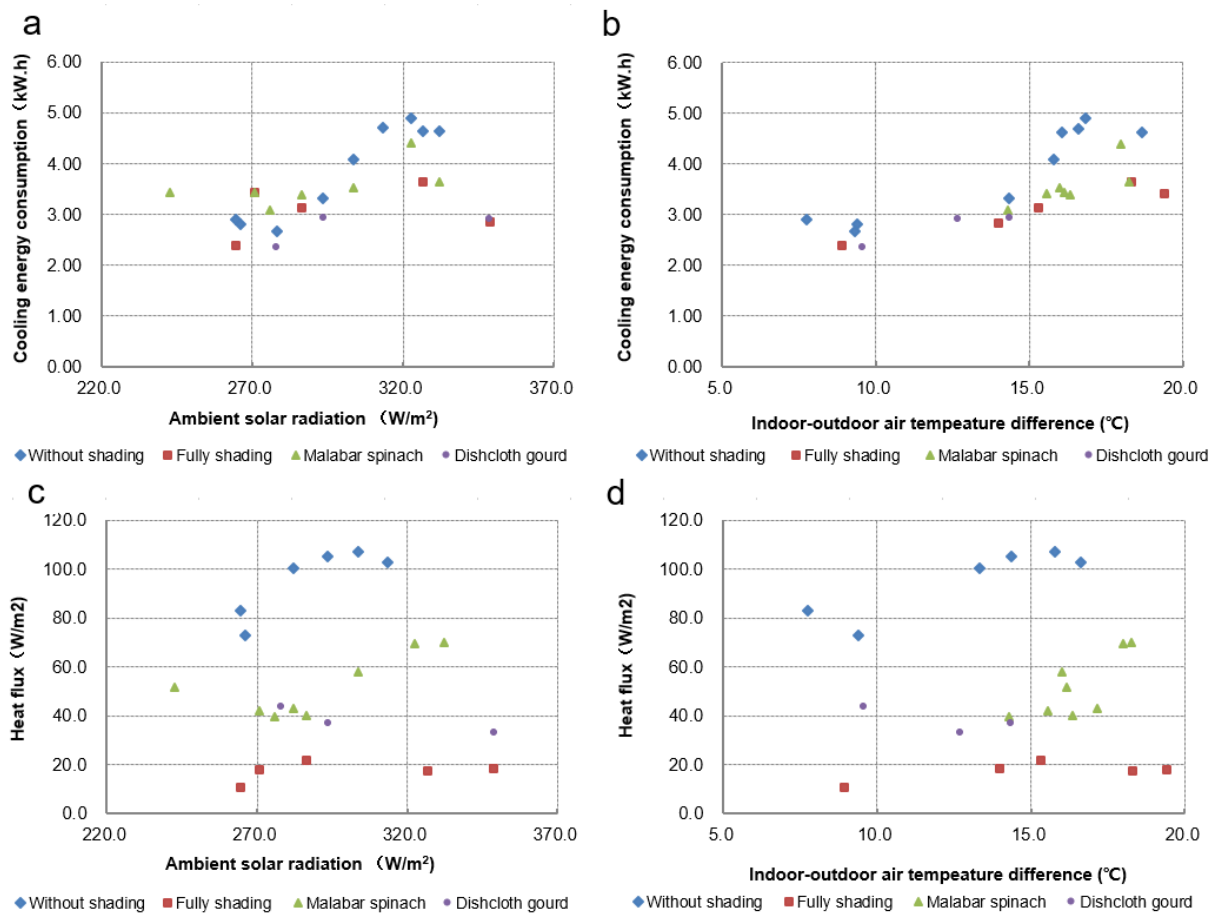
Fig. 10. Scatterplot of averaged (a) solar radiation and cooling energy consumption, (b) indoor-outdoor air temperature difference and cooling energy consumption, (c) solar radiation and heat flux, and (d) indoor-outdoor air temperature difference and heat flux

Table 2. Correlation coefficients between the cooling energy consumption and climatic factors

	Cooling energy consumption		
	Without shading	Fully shading	Green shading (Malabar spinach)
Ambient solar radiation (on the west vertical plane)	0.94	0.24	0.61
Indoor-outdoor air temperature difference	0.92	0.96	0.79

Table 3. Correlation coefficients between the heat flux and Climatic factors

	Heat flux		
	Without shading	Fully shading	Green shading (Malabar spinach)
Ambient solar radiation (on the west vertical plane)	0.85	0.36	0.73
Indoor-outdoor air temperature difference	0.89	0.66	0.75

4.1.2 Performance of green shading

Based on the data obtained between 12:00-18:00 PM from a sunny day (August 28), a detailed analysis on the performance of the green shading is conducted. On that day, the test room was equipped with Dishcloth gourd shading and the reference room without shading. Fig. 11 shows the instantaneous indoor and outdoor air temperatures and heat flux transferred through the window glass. It indicates that the indoor air temperatures suffered from fluctuation, while the time-averaged indoor air temperatures of the two rooms were kept close to each other by 22.7 C° by the air conditioners. The measured heat fluxes transferred through the window glass of the two rooms are illustrated in Fig. 11. It can be seen that the strong heat flux transferred through the window without shading reached a maximum of 147 W/m^2 at 16:00 PM. For the window with green shading, less transmitted heat flux was observed, and the peak hour was observed between 14:00 and 15:00 PM. Table 4 summarises the cooling energy consumption and average transmitted heat flux of the windows in two rooms, and the percentage reduction by green shading. It shows that cooling energy consumption was reduced by 11.45%, and the heat flux transferred through the window glass was reduced by 64.84%.

The reduction of transmitted heat flux and cooling energy consumption presented above mainly came from the interception of solar radiation by the plant canopy, e.g. the shading effects. The following sections will investigate the shading performance using C_s.

Table 4. The measured data of the two rooms and reduction by green shading (averaged from 12:00 to 18:00 PM)

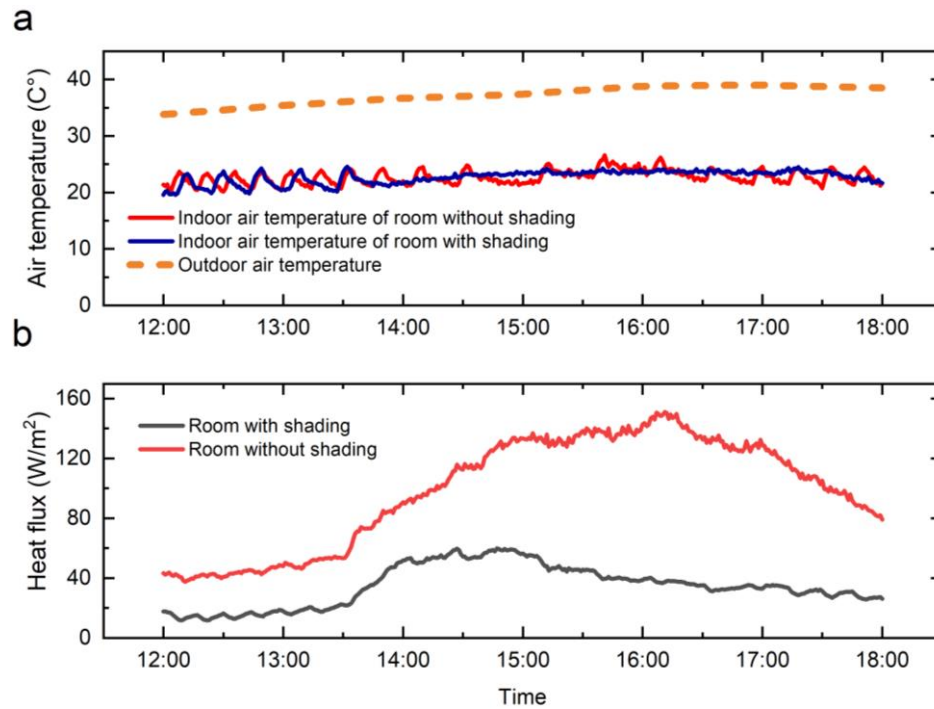|	Room without shading	Room with shading	Reduction percentage
Cooling energy consumption (kWh)	3.32	2.94	11.45%
Average transmitted heat flux through the window glass(W/m^2)	98.7	34.7	64.84%

Fig. 11. Measured instantaneous (a) indoor and outdoor air temperatures and (b) transmitted heat flux on August 28.

4.2 Impact of coverage rates on shading coefficients

The experiment of the shading coefficient for the west-facing windows was conducted in the process of plant growth from August to October. Data from sunny days were picked out to explore the correlation between coverage rates (C_r) and shading coefficient (C_s). Using the approach described in Section 3.4.5, the C_r was extracted from the pictures. The values of surface-averaged shading coefficients ($C_{s.s.avg}$) were calculated using Eq. (3) and averaged on a daily basis. The obtained $C_{s.s.avg}$ and C_r are scattered in Fig. 12. Given that zero coverage rate (0%) always yielded $C_{s.s.avg}$ value of 1, one point was added for each case (the top left corner of Figs. 12a, b, and c). On the basis of these points, strong exponential correlations were obtained. The regression equations for the three species are expressed as follows:

Dishcloth gourd: $C_{s.s.avg} = 1.0081e^{-0.016C_r}$ ($R^2 = 0.958$) (8)

Malabar spinach: $\quad C_{s.s.avg} = 0.9165e^{-0.0184C_r}$ ($R^2 = 0.984$) $\qquad$ (9)

Morning glory: $\quad C_{s.s.avg} = 1.0264e^{-0.0204C_r}$ ($R^2 = 0.986$) $\qquad$ (10)
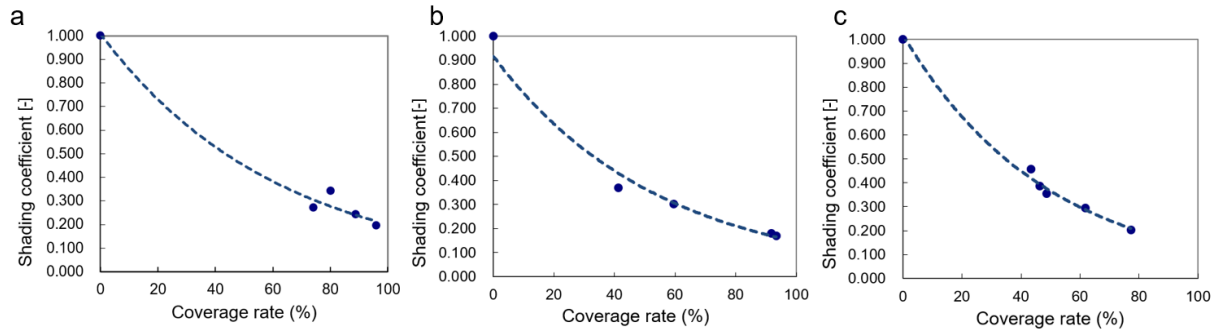

Fig. 12. Shading coefficient for different coverage rates and exponential regression of (a) Dishcloth gourd, (b) Malabar spinach, and (c) Morning glory.

Based on the equations above, the C_s can be easily calculated with the measured C_r for the three species. On August 28, the measured C_r of Dishcloth gourd was 80%. Based on equation (8), the C_s was 0.28, and the corresponding reduction of cooling energy consumption and heat flux transferred through the window glass were 11.45% and 64.84%, respectively (Table 4).

4.3 Impact of solar radiation and solar angle on shading coefficient

The results above summarized a general feature of green shading. In the following sections, detailed characteristics of the three species will be investigated using instantaneous data.

4.3.1 Solar tracking experiment

Fig. 13a shows the shading coefficient, ambient solar radiation, and solar radiation behind green shading obtained from the solar tracking experiment for Dishcloth gourd on August 14. The solar radiation on the vertical surface decreased from 10:00 AM, reached the minimum and then increased. The turning point was at noon around 13:20 PM. The measured shading coefficient showed the opposite tendency, which increased from 10:00 AM in the morning and decreased from 13:20 PM in the afternoon. The maximum shading coefficient was observed at noon. Fig. 13b illustrates the scatterplot of shading coefficient and ambient solar radiation, which are colored by two phases depending on the ascending and the descending of solar radiation. In general, solar radiation was negatively correlated with the shading coefficient. In addition, no evident difference was found between the ascending phase (before 13:20 PM) and the descending phase (after 13:20 PM).
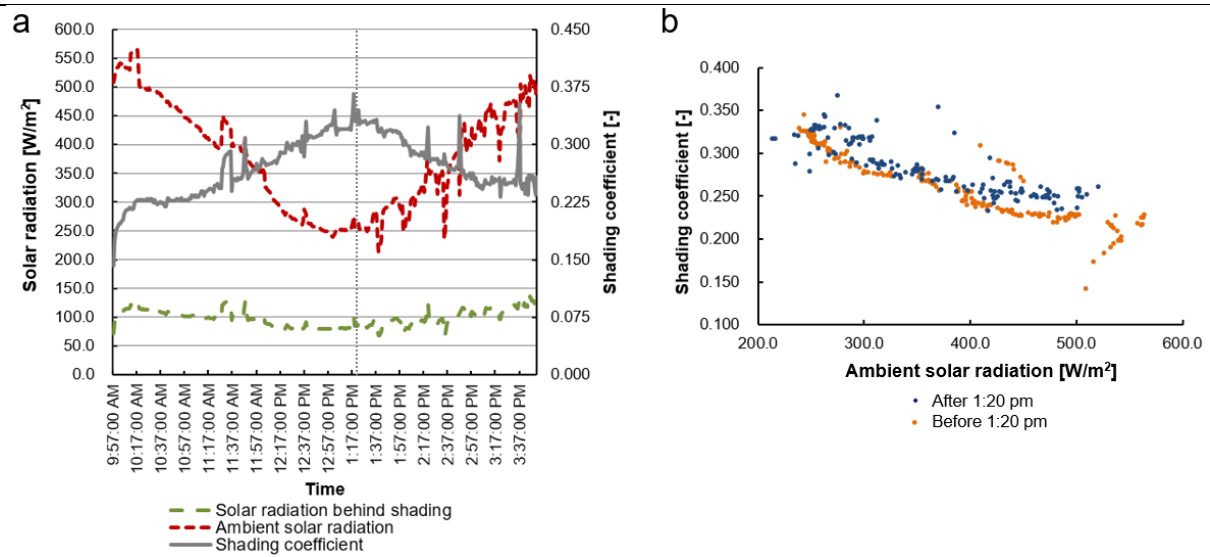
Fig. 13. Measured (a) instantaneous surface-averaged shading coefficient, ambient solar radiation, and solar radiation behind the green shading; (b) scatterplot of shading coefficient and ambient solar radiation on August 14 from solar tracking experiment.

On sunny days, solar radiation received on a façade depends on the angle between the direct sunlight and the surface (Mingfang, 2002). For common shading devices with a fixed geometry, the instantaneous shading coefficient is changing with the solar position. It is possible that there is a similar tendency exists for green shading. In this case, we explored the relationship between the green shading coefficient and the solar position. The solar position relevant to the MGWSS model can be qualified by two angles: (1) the solar altitude (namely α) and (2) the angle between the solar azimuth and the surface normal of MGWSS plane (namely β) (see Fig. 14b). In the solar tracking experiment, the orientation was turned every half hour to follow the sun. Note that it could not control the MGWSS model always exactly perpendicular to the solar azimuth angle, but it keeps β very small. Therefore, the solar position was mainly decided by the altitude (α) during this solar tracking experiment. Fig. 14a shows the measured shading coefficient and altitude (α) on August 14. α was calculated according to the date and location. It indicates that high α generally led to large shading coefficient, which means the solar shading ability was weaker for the sun at a higher altitude than at a lower altitude.
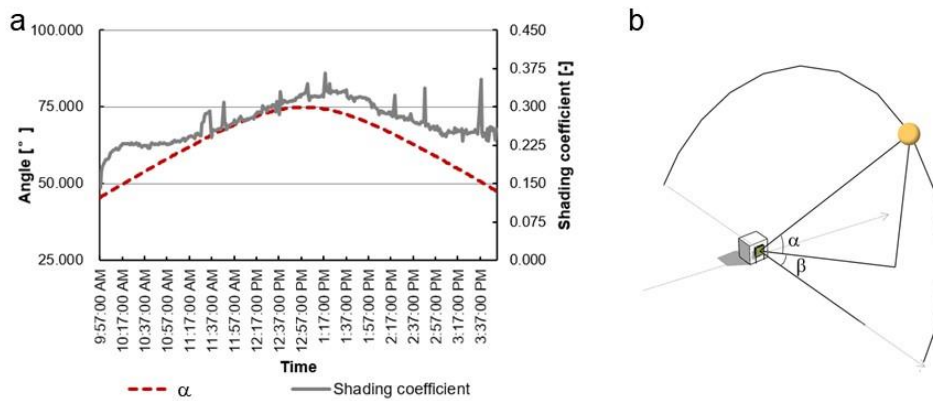
Fig. 14. (a) Measured instantaneous surface-averaged shading coefficient and α on August 14 from solar tracking experiment and (b) definitions of altitude (α) and the angle between the solar azimuth and the surface normal of MGWSS (β)

4.3.2 Experiment for west-facing windows

Measured data from the experiment of the shading coefficient for west-facing windows were used for investigation. The successive sunny days from October 6, 7 and 8 were suitable for comparative study. Experiments on October 6, 7, and 8 were conducted for Malabar spinach, Dishcloth gourd, and Morning glory, respectively. Fig. 15 illustrates the status of the three species in this experiment. Figs. 16a, c, and e show the measured shading coefficient, ambient solar radiation, and surface-averaged solar radiation behind the green shading. They indicated that the ambient solar radiation on the west wall first rose and then declined. The peak solar radiation was observed between 15:00 PM and 16:00 PM.
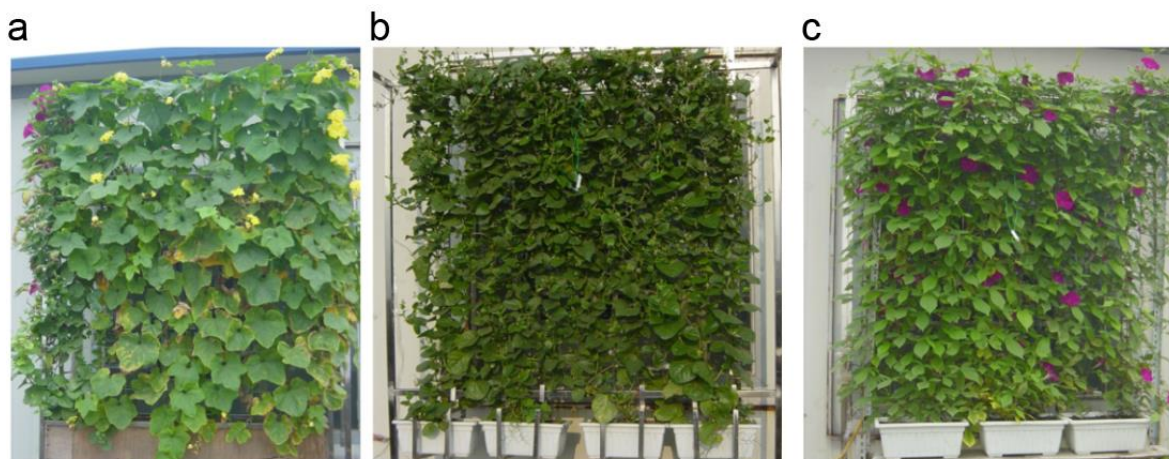

Fig. 15. Status of the three species in the experiment for west-facing windows: (a) Dishcloth gourd on October 8, (b) Malabar spinach on October 6, and (c) Morning glory on October 7.
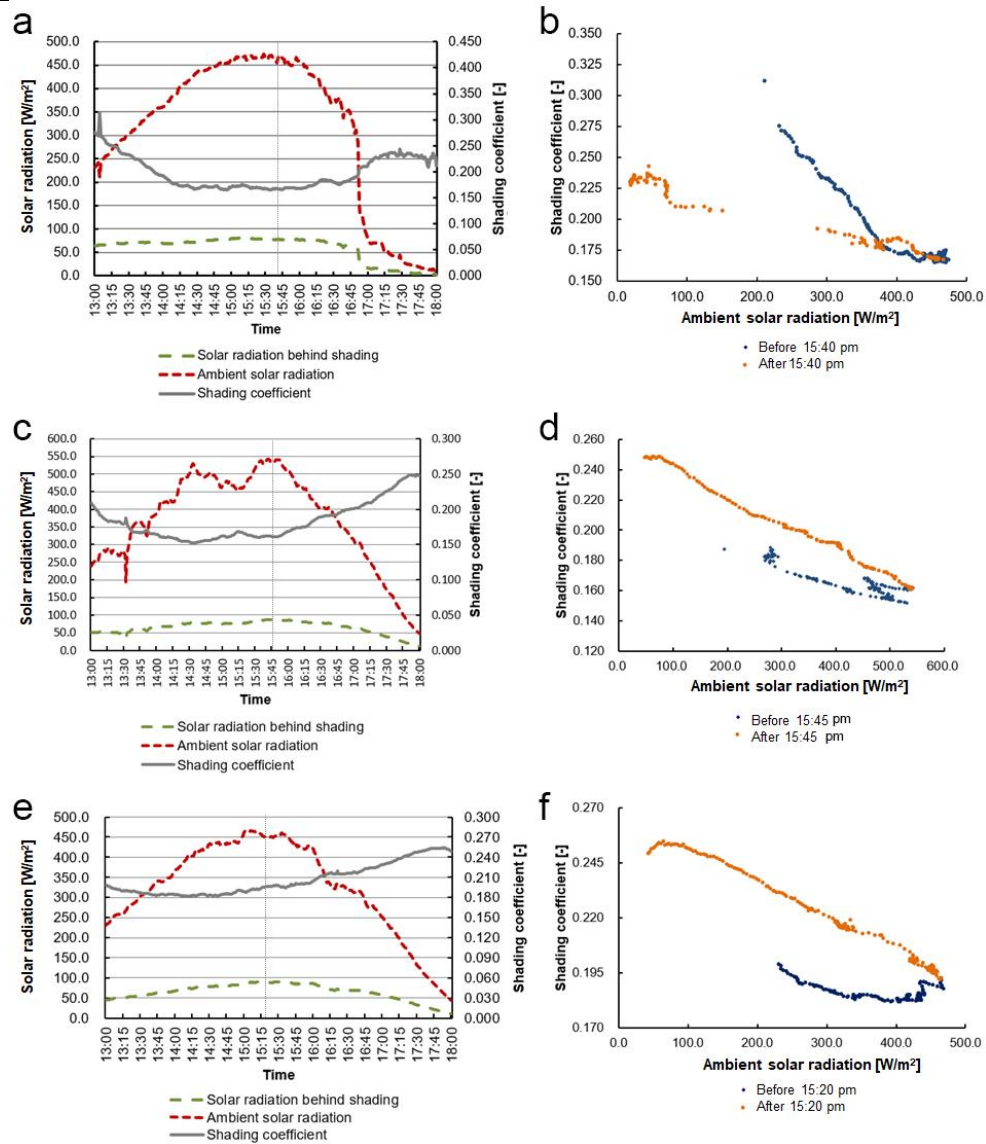
Fig. 16. Measured results from the shading experiment for west-facing windows: (a) instantaneous surface-averaged shading coefficient, ambient solar radiation, and solar radiation behind the green shading; (b) scatter plot of shading coefficient and ambient solar radiation for Dishcloth gourd in the on October 8. (c-d) same for Malabar spinach on October 6: (e-f) same for Morning glory on October 7

Figs. 16b, d, and f illustrate the scatterplots of the shading coefficient and ambient solar radiation. The data are colored by the two phases depending on the ascending and descending of solar radiation, which is divided by the approximate turning points (shown by the dashed line).

Generally, stronger solar radiation led to better shading performance (lower shading coefficient). This was the same as the solar tracking experiment, and generally in line with a past experimental finding that the surface cooling effect by a green facade increases with solar radiation (Kokogiannakis et al., 2019). However, large discrepancies were observed between the ascending and descending phases when solar radiation was the same. For Dishcloth gourd, lower $C_{s.s.avg}$ was observed at the descending phase

than at the ascending phase (Fig. 16b). By contrast, larger $C_{s.s.avg}$ was found at the descending phase than at the ascending phase for Malabar spinach and Morning glory (Figs. 16d and f). The possible reason is that the solar position was different when solar radiation was the same.
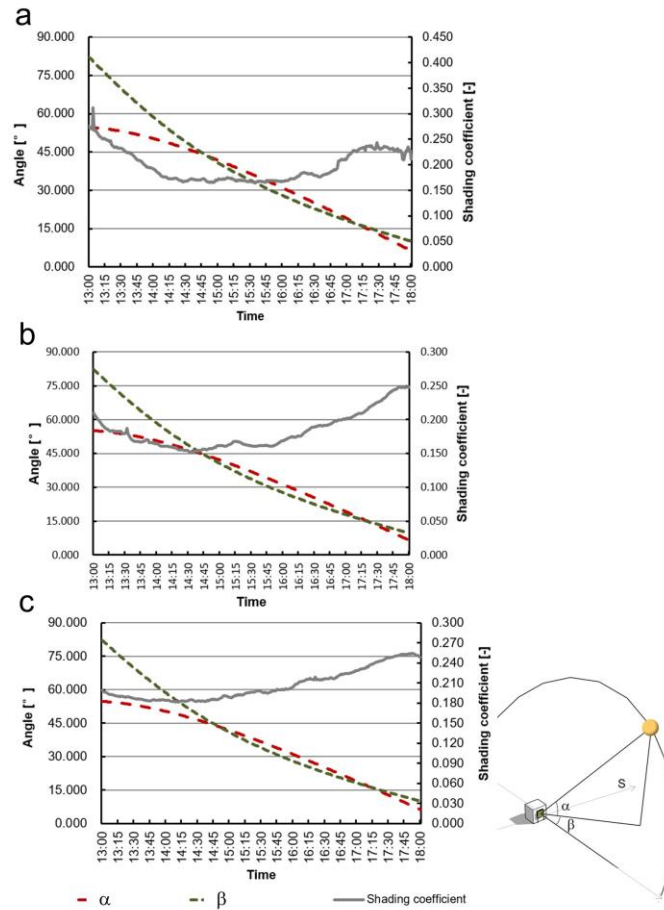

Fig. 17. Measured instantaneous surface-averaged shading coefficient, α, and β of (a) Dishcloth gourd on October 8, (b) Malabar spinach on October 6, (c) Morning glory on October 7, from the experiments for west-facing windows.

As mentioned in Section 4.3.1, solar radiation on a façade on sunny days depends on α and β, which were calculated according to the experimental date and time. Figs. 17a-c show the measured shading coefficient, α, and β in shading experiment for the west-facing windows for Dishcloth gourd, Malabar spinach, and Morning glory, respectively. The measurement started at 13:00 PM. At this time, β was approximately 83°, and a low ambient solar radiation on the west surface is observed (also see in Figs. 16a c and e). The shading coefficients of the three species decreased first and then increased. For example, $C_{s.s.avg}$ of Dishcloth gourd stopped decreasing and stabilized at 14:15 PM when α and β were 48° and 53°, respectively, then, increased at 16:10 when α and β reached 30° and 25°, respectively. For

Malabar spinach and Morning glory, the points of turning up were observed at a high angle: the turning points of α were 46° and 55°, and β were 46° and 48°, respectively.

These results demonstrated that the lowest shading coefficient was found at an oblique solar incidence angle. When the solar position approaching the west, which means α and β approaching 0°, the shading coefficient increased. In this case, Malabar spinach and Morning glory were more sensitive than Dishcloth gourd that had low $C_{s.s.avg}$ in the second phase (Fig. 16b). It indicated that Dishcloth gourd had a stronger shading ability for perpendicular sunlight than the two other species.

4.4 Distribution of shading coefficients for west-facing windows

Local solar radiation behind green shading (E_i) was measured by the 35 PV panels. $C_{s.loc}$ was calculated by substituting local E_i into Eq. (2). Similar to Section 4.3.2, data from October 6 to 8 were applied for analysis. Fig. 18 shows the distribution of the time-averaged shading coefficient of the three species. Note that the data from each PV panel is shown by one point in this figure, therefore, 5×7 points in total. The surface-averaged shading coefficients ($C_{s.s.avg}$) were 0.204, 0.189, and 0.201 with standard deviation (SD) of 0.024, 0.011, and 0.025 for Dishcloth gourd, Malabar spinach, and Morning glory, respectively (Table 5). It indicated the strong inhomogeneous distribution of shading coefficients for Dishcloth gourd and Morning glory.
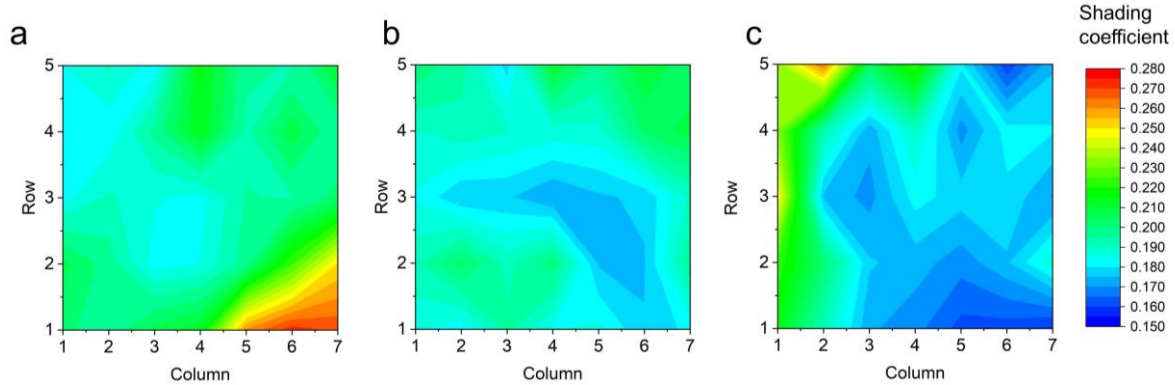

Fig. 18. Distribution of time-averaged shading coefficients for (a) Dishcloth gourd on October 8, (b) Malabar spinach on October 6, and (c) Morning glory on October 7.

Table 5. $C_{s.s.avg}$ and SD

	Dishcloth gourd	Malabar spinach	Morning glory
$C_{s.s.avg}$	0.204	0.189	0.201
SD	0.024	0.011	0.025

The row averaged C_s values of the three species were calculated. Fig. 19 shows the hourly data from 12:00 PM to 17:00 PM. For Dishcloth gourd at the early hours, the lower row yielded a higher C_s,

where the tendency became unclear after 14:00 (Fig. 19a). For Malabar spinach, the lower row mostly had a lower C_s (Fig. 19b). For Morning glory, it was obvious that the lower row yielded the lower C_s before 15:00 PM (Fig. 19c).
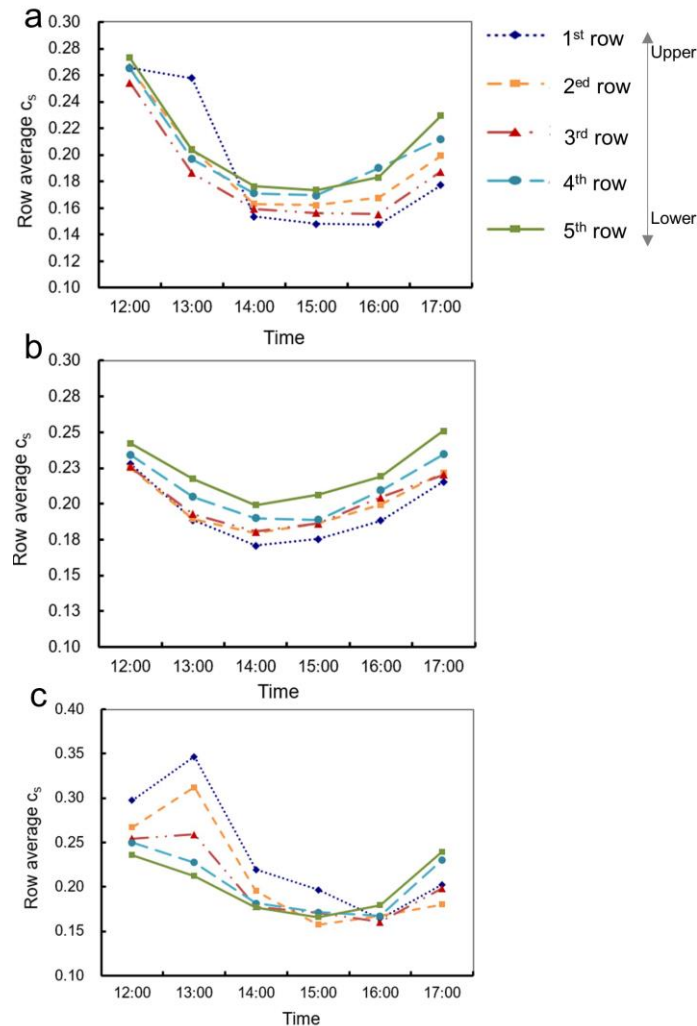

Fig. 19. Hourly row averaged C_s of (a) Dishcloth gourd on October 8, (b) Malabar spinach on October 6 and (c) Morning glory on October 7.

5. Discussion and limitation

The vast majority of the existing studies had focused on the implementation of vertical greenery systems for opaque building walls rather than windows. The possible reason was that vertical greenery may block the view and reduce daylight and natural ventilation, which contradicts with the function of the windows. In this perspective, Stec et al. proposed design of flowerpot on rotating slats (Stec et al., 2005), Lee and Jim raised an idea of rotatable green wall planter system design (Lee and Jim, 2019). The present study proposed a concept of movable green window shading systems (MGWSS), and simplified models that represent the MGWSS under shading status were built for the experiment. The

shading coefficient of three plants obtained in this study is applicable to similar green shading for windows.

The density of the foliage is an uncertain but important parameter related to the performance of green shading. Coverage rate (C_r) represents the 2D behavior of foliage, while the 3D behavior is related to the angle of leaves and the number of leaf layers. During the growth of the plant, the leaves gradually increase and always grow towards the sunlight, which increases the C_r and also the complexity of its 3D structure. Therefore, the 3D behavior of foliage is related to C_r, i.e. when the C_r is high, the number of layers of foliage leaves is also large. It decreased the solar radiation passing through the foliage (shown Fig. 12), which is in line with the past study (Ip et al., 2010) that solar transmissivity reduced with the increase of the number of leaf layers. As mentioned in the introduction, LAI is another index to qualify the foliage density, which was assumed in some numerical studies to simulate the effect of foliage (Flores Larsen et al., 2015; Susorova et al., 2013). Further study could investigate the relationship between C_r (represents the 2D behavior of foliage) and LAI (represents the 3D behavior of foliage).

The experiments of cooling energy consumption and heat flux focus on a window at the west orientation. Previous studies on green façades show that the performance is also good for east and south orientations. This could be the case for windows. Further study should evaluate the other orientations, the impact of other climatic factors, e.g. cloud coverage, and also the effects on energy saving under the other shading status, indoor thermal comfort, interior daylighting and natural ventilation.

6. Conclusions

In this study, a concept of MGWSS was proposed. A new onsite measurement technique was developed to examine the shading performance of MGWSS. Experiments were conducted to measure the coverage rate, shading coefficient, heat flux reduction, and cooling energy saving. The main findings are summarized as follows:

1. The presence of green shading reduced the impact of solar radiation and indoor-outdoor air temperature difference on the cooling energy consumption. It is found that the correlation coefficient (C_c) between cooling energy consumption and ambient solar radiation was reduced from 0.94 to 0.61 by the green shading, and the C_c between cooling energy consumption and indoor-outdoor air temperature difference was reduced from 0.92 to 0.79.

2. Distribution of solar radiation on a surface behind green shading could be indirectly measured by PV panels with acceptable accuracy; shading coefficients of green shading could be calculated correspondingly.

3. Equations between the C_r and C_s are established for the three species, respectively. Based on the equations, the C_s can be easily calculated with the measured C_r. When the C_r was 80%, the C_s was

0.28, which leads to the reduction of cooling energy consumption and heat flux transmitted through the glass of the west-facing window by 11.45% and 64.84% in an afternoon.

4. For the west-facing window, the characteristics of shading coefficients were different during the ascending and descending phases of solar radiation. The lowest shading coefficient was found at oblique solar incidence angles around 14:00–16:00 PM, then, the shading coefficient increased when the solar position approached the west.

5. Inhomogeneous distribution of shading coefficients was found. The surface-averaged C_s values were 0.204, 0.189, and 0.201 with standard deviations of 0.024, 0.011, and 0.025 for Dishcloth gourd, Malabar spinach, and Morning glory, respectively.

Acknowledgment

Reference

Abhijith, K.V., Kumar, P., Gallagher, J., McNabola, A., Baldauf, R., Pilla, F., Broderick, B., Di Sabatino, S., Pulvirenti, B., 2017. Air pollution abatement performances of green infrastructure in open road and built-up street canyon environments – A review. Atmos. Environ. 162, 71–86. https://doi.org/10.1016/J.ATMOSENV.2017.05.014

Alexandri, E., Jones, P., 2008. Temperature decreases in an urban canyon due to green walls and green roofs in diverse climates. Build. Environ. 43, 480–493. https://doi.org/10.1016/J.BUILDENV.2006.10.055

Bustami, R.A., Belusko, M., Ward, J., Beecham, S., 2018. Vertical greenery systems: A systematic review of research trends. Build. Environ. 146, 226–237. https://doi.org/10.1016/J.BUILDENV.2018.09.045

Chartered Institution of Building Services Engineers., 2006. Environmental design: CIBSE guide A., 7th ed. Chartered Inst. of Building Services Engineers, London.

Cuce, E., 2017. Thermal regulation impact of green walls: An experimental and numerical investigation. Appl. Energy 194, 247–254. https://doi.org/10.1016/J.APENERGY.2016.09.079

Dahanayake, K.C., Chow, C.L., Long Hou, G., 2017. Selection of suitable plant species for energy efficient Vertical Greenery Systems (VGS). Energy Procedia 142, 2473–2478. https://doi.org/10.1016/J.EGYPRO.2017.12.185

David, M., Donn, M., Garde, F., Lenoir, A., 2011. Assessment of the thermal and visual efficiency of solar shades. Build. Environ. 46, 1489–1496. https://doi.org/10.1016/J.BUILDENV.2011.01.022

De Masi, R.F., de Rossi, F., Ruggiero, S., Vanoli, G.P., 2019. Numerical optimization for the design of living walls in the Mediterranean climate. Energy Convers. Manag. 195, 573–586.

https://doi.org/10.1016/J.ENCONMAN.2019.05.043

Ebrahimpour, A., Maerefat, M., 2011. Application of advanced glazing and overhangs in residential buildings. Energy Convers. Manag. 52, 212–219. https://doi.org/10.1016/J.ENCONMAN.2010.06.061

Eumorfopoulou, E.A., Kontoleon, K.J., 2009. Experimental approach to the contribution of plant-covered walls to the thermal behaviour of building envelopes. Build. Environ. 44, 1024–1038. https://doi.org/10.1016/J.BUILDENV.2008.07.004

Feng, H., Hewage, K., 2014. Lifecycle assessment of living walls: air purification and energy performance. J. Clean. Prod. 69, 91–99. https://doi.org/10.1016/J.JCLEPRO.2014.01.041

Flores Larsen, S., Filippín, C., Lesino, G., 2015. Modeling double skin green façades with traditional thermal simulation software. Sol. Energy 121, 56–67. https://doi.org/10.1016/J.SOLENER.2015.08.033

Haldi, F., Robinson, D., 2010. Adaptive actions on shading devices in response to local visual stimuli. J. Build. Perform. Simul. 3, 135–153. https://doi.org/10.1080/19401490903580759

Hamdan, M.A., 1994. Thermal gains through windows. Energy Convers. Manag. 35, 501–506. https://doi.org/10.1016/0196-8904(94)90091-4

Hoelscher, M.-T., Nehls, T., Jänicke, B., Wessolek, G., 2016. Quantifying cooling effects of facade greening: Shading, transpiration and insulation. Energy Build. 114, 283–290. https://doi.org/10.1016/J.ENBUILD.2015.06.047

Hoyano, A., 1988. Climatological uses of plants for solar control and the effects on the thermal environment of a building. Energy Build. 11, 181–199. https://doi.org/10.1016/0378-7788(88)90035-7

Huang, Z., Lu, Y., Wong, N.H., Poh, C.H., 2019. The true cost of "greening" a building: Life cycle cost analysis of vertical greenery systems (VGS) in tropical climate. J. Clean. Prod. 228, 437–454. https://doi.org/10.1016/J.JCLEPRO.2019.04.275

Imran, H.M., Kala, J., Ng, A.W.M., Muthukumaran, S., 2018. Effectiveness of green and cool roofs in mitigating urban heat island effects during a heatwave event in the city of Melbourne in southeast Australia. J. Clean. Prod. 197, 393–405. https://doi.org/10.1016/J.JCLEPRO.2018.06.179

Ip, K., Lam, M., Miller, A., 2010. Shading performance of a vertical deciduous climbing plant canopy. Build. Environ. 45, 81–88. https://doi.org/10.1016/J.BUILDENV.2009.05.003

Ip, K., Marta, L., Miller, A., 2004. Bioshaders for sustainable buildings. CIB 2004 World Building Congress, Toronto, Canada.

Jim, C.Y., 2015. Thermal performance of climber greenwalls: Effects of solar irradiance and orientation. Appl. Energy 154, 631–643. https://doi.org/10.1016/J.APENERGY.2015.05.077

Kirimtat, A., Koyunbaba, B.K., Chatzikonstantinou, I., Sariyildiz, S., 2016. Review of simulation modeling for shading devices in buildings. Renew. Sustain. Energy Rev. 53, 23–49. https://doi.org/10.1016/J.RSER.2015.08.020

Kokogiannakis, G., Darkwa, J., Badeka, S., Li, Y., 2019. Experimental comparison of green facades with outdoor test cells during a hot humid season. Energy Build. 185, 196–209. https://doi.org/10.1016/J.ENBUILD.2018.12.038

Kontoleon, K.J., Eumorfopoulou, E.A., 2010. The effect of the orientation and proportion of a plant-covered wall layer on the thermal performance of a building zone. Build. Environ. 45, 1287–1303. https://doi.org/10.1016/J.BUILDENV.2009.11.013

Koyama, T., Yoshinaga, M., Hayashi, H., Maeda, K., Yamauchi, A., 2013. Identification of key plant traits contributing to the cooling effects of green façades using freestanding walls. Build. Environ. 66, 96–103. https://doi.org/10.1016/J.BUILDENV.2013.04.020

Koyama, T., Yoshinaga, M., Maeda, K., Yamauchi, A., 2015. Transpiration cooling effect of climber green wall with an air gap on indoor thermal environment. Ecol. Eng. 83, 343–353. https://doi.org/10.1016/J.ECOLENG.2015.06.015

Lee, L.S.H., Jim, C.Y., 2019. Transforming thermal-radiative study of a climber green wall to innovative engineering design to enhance building-energy efficiency. J. Clean. Prod. 224, 892–904. https://doi.org/10.1016/J.JCLEPRO.2019.03.278

Ling, T.-Y., Chiang, Y.-C., 2018. Well-being, health and urban coherence-advancing vertical greening approach toward resilience: A design practice consideration. J. Clean. Prod. 182, 187–197. https://doi.org/10.1016/J.JCLEPRO.2017.12.207

Mingfang, T., 2002. Solar control for buildings. Build. Environ. 37, 659–664. https://doi.org/10.1016/S0360-1323(01)00063-4

Palmero-Marrero, A.I., Oliveira, A.C., 2010. Effect of louver shading devices on building energy requirements. Appl. Energy 87, 2040–2049. https://doi.org/10.1016/J.APENERGY.2009.11.020

Pan, L., Wei, S., Chu, L.M., 2018. Orientation effect on thermal and energy performance of vertical greenery systems. Energy Build. 175, 102–112. https://doi.org/10.1016/J.ENBUILD.2018.07.024

Papadakis, G., Tsamis, P., Kyritsis, S., 2001. An experimental investigation of the effect of shading with plants for solar control of buildings. Energy Build. 33, 831–836. https://doi.org/10.1016/S0378-7788(01)00066-4

Pérez, G., Coma, J., Martorell, I., Cabeza, L.F., 2014a. Vertical Greenery Systems (VGS) for energy saving in buildings: A review. Renew. Sustain. Energy Rev. 39, 139–165. https://doi.org/10.1016/J.RSER.2014.07.055

Pérez, G., Coma, J., Martorell, I., Cabeza, L.F., 2014b. Vertical Greenery Systems (VGS) for energy saving in buildings: A review. Renew. Sustain. Energy Rev. 39, 139–165. https://doi.org/10.1016/J.RSER.2014.07.055

Pérez, G., Rincón, L., Vila, A., González, J.M., Cabeza, L.F., 2011. Behaviour of green facades in Mediterranean Continental climate. Energy Convers. Manag. 52, 1861–1867. https://doi.org/10.1016/J.ENCONMAN.2010.11.008

Pérez, G., Rincón, L., Vila, A., González, J.M., Cabeza, L.F., 2011. Green vertical systems for buildings as passive systems for energy savings. Appl. Energy 88, 4854–4859.

https://doi.org/10.1016/J.APENERGY.2011.06.032

Perini, K., Ottelé, M., Fraaij, A.L.A., Haas, E.M., Raiteri, R., 2011. Vertical greening systems and the effect on air flow and temperature on the building envelope. Build. Environ. 46, 2287–2294. https://doi.org/10.1016/J.BUILDENV.2011.05.009

Perini, K., Ottelé, M., Haas, E.M., Raiteri, R., 2013. Vertical greening systems, a process tree for green façades and living walls. Urban Ecosyst. 16, 265–277. https://doi.org/10.1007/s11252-012-0262-3

Perini, K., Rosasco, P., 2013. Cost–benefit analysis for green façades and living wall systems. Build. Environ. 70, 110–121. https://doi.org/10.1016/J.BUILDENV.2013.08.012

Safikhani, T., Abdullah, A.M., Ossen, D.R., Baharvand, M., 2014. A review of energy characteristic of vertical greenery systems. Renew. Sustain. Energy Rev. 40, 450–462. https://doi.org/10.1016/J.RSER.2014.07.166

Singh, R., Lazarus, I.J., Kishore, V.V.N., 2016. Uncertainty and sensitivity analyses of energy and visual performances of office building with external venetian blind shading in hot-dry climate. Appl. Energy 184, 155–170. https://doi.org/10.1016/J.APENERGY.2016.10.007

Skoplaki, E., Palyvos, J.A., 2009. On the temperature dependence of photovoltaic module electrical performance: A review of efficiency/power correlations. Sol. Energy 83, 614–624. https://doi.org/10.1016/J.SOLENER.2008.10.008

Stec, W.J., van Paassen, A.H.C., Maziarz, A., 2005. Modelling the double skin façade with plants. Energy Build. 37, 419–427. https://doi.org/10.1016/J.ENBUILD.2004.08.008

Sudimac, B., Ilić, B., Munćan, V., Anđelković, A.S., 2019. Heat flux transmission assessment of a vegetation wall influence on the building envelope thermal conductivity in Belgrade climate. J. Clean. Prod. 223, 907–916. https://doi.org/10.1016/J.JCLEPRO.2019.02.087

Sunakorn, P., Yimprayoon, C., 2011. Thermal Performance of Biofacade with Natural Ventilation in the Tropical Climate. Procedia Eng. 21, 34–41. https://doi.org/10.1016/J.PROENG.2011.11.1984

Susorova, I., Angulo, M., Bahrami, P., Brent Stephens, 2013. A model of vegetated exterior facades for evaluation of wall thermal performance. Build. Environ. 67, 1–13. https://doi.org/10.1016/J.BUILDENV.2013.04.027

Susorova, I., Azimi, P., Stephens, B., 2014. The effects of climbing vegetation on the local microclimate, thermal performance, and air infiltration of four building facade orientations. Build. Environ. 76, 113–124. https://doi.org/10.1016/J.BUILDENV.2014.03.011

Tang, M., Zheng, X., 2019. Experimental study of the thermal performance of an extensive green roof on sunny summer days. Appl. Energy 242, 1010–1021. https://doi.org/10.1016/j.apenergy.2019.03.153

Wong, N.H., Kwang Tan, A.Y., Chen, Y., Sekar, K., Tan, P.Y., Chan, D., Chiang, K., Wong, N.C., 2010. Thermal evaluation of vertical greenery systems for building walls. Build. Environ. 45, 663–672. https://doi.org/10.1016/J.BUILDENV.2009.08.005

Wong, N.H., Tan, A.Y.K., Tan, P.Y., Wong, N.C., 2009. Thermal evaluation of vertical greenery systems for building walls. Energy Build. 41, 1401–1408. https://doi.org/10.1016/J.ENBUILD.2009.08.010

Yang, A.-S., Juan, Y.-H., Wen, C.-Y., Chang, C.-J., 2017. Numerical simulation of cooling effect of vegetation enhancement in a subtropical urban park. Appl. Energy 192, 178–200. https://doi.org/10.1016/J.APENERGY.2017.01.079

Zaid, S.M., Perisamy, E., Hussein, H., Myeda, N.E., Zainon, N., 2018. Vertical Greenery System in urban tropical climate and its carbon sequestration potential: A review. Ecol. Indic. 91, 57–70. https://doi.org/10.1016/J.ECOLIND.2018.03.086